Fermi National Accelerator Laboratory

FERMILAB-Conf-98/160-E
CDF

Rare B Decays, Mixing and CP Violation at Tevatron

J. Suzuki
For the CDF Collaboration

Fermi National Accelerator Laboratory
P.O. Box 500, Batavia, Illinois 60510

June 1998

Published Proceedings of the *33rd Rencontres de Moriond: QCD and High Energy Hadronic Interactions*, Les Arcs, France, March 21-28, 1998

Operated by Universities Research Association Inc. under Contract No. DE-AC02-76CH03000 with the United States Department of Energy

Disclaimer

Distribution

Rare b decays, mixing and CP violation at Tevatron
(Rare b decays and Observation of B_c^+ Mesons at Tevatron)

Jun-ichi SUZUKI
Institute of Physics, University of Tsukuba, 1-1-1 Tennoudai,
Tsukuba Ibaraki 305, Japan [a]

We report the results of the search for flavor changing-neutral current (FCNC) decays $b \to s\mu^+\mu^-$ and the observation of B_c^+ mesons at Tevatron.

1 Search for the flavor-changing neutral-current decays $b \to s\mu^+\mu^-$

The flavor-changing neutral-current (FCNC) decays $b \to s\ell^+\ell^-$ are forbidden at the tree level diagram. They can proceed through the higher order diagrams, *i.e.*, penguin and box diagrams which include one loop. These diagrams are sensitive to CKM-matrix element V_{ts}, and are also sensitive to new physics, since charged Higgs bosons, new gage bosons or supersymetric particles can contribute through the loop. The Standard Model prediction [1] for the branching fraction of $b \to s\ell^+\ell^-$ is $\mathcal{O}(10^{-6})$. The dilepton pair can be resonant, for example, J/ψ and $\psi(2S)$. They are not distinguishable from the internal spectator decay, $b \to cW^- \to c\bar{c}s$. We search for non-resonant part of dilepton mass spectrum. CDF and DØ search for the FCNC decays of $b \to s\mu^+\mu^-$ modes which can be triggered easily at a hadron collider due to their dimuon signature.

1.1 Search for Inclusive FCNC decays $b \to X_s\mu^+\mu^-$ in DØ

DØ searches for the inclusive FCNC decays $b \to X_s\mu^+\mu^-$ in data (50 pb^{-1}) which are collected by the dimuon trigger [2]. Dimuon candidates are required to be oppositely charged muon pair with the invariant mass $m(\mu^+\mu^-) < 7$ GeV/c^2, transverse momentum $p_T(\mu^+\mu^-) > 5$ GeV/c and pseudo-rapidity $|\eta(\mu^+\mu^-)| < 0.6$. The both muons are also required to have $p_T(\mu^\pm) > 3.5$ GeV/c and $|\eta(\mu^\pm)| < 1.0$. The dimoun invariant mass satisfying these requirements are shown in Fig. 1.

The search is performed in the window $3.9 < m(\mu^+\mu^-) < 4.9$ GeV/c^2. They fit the dimuon invariant mass distribution to these know sources: (1) J/ψ and $\psi(2S)$ signal, (2) double semileptonic decays of $b\bar{b}$ and $c\bar{c}$ events, (3) a sequential semileptonic decay of b hadron (4) one muon comes from a true semileptonic decay of b or c quark and the other from K^+ or π^+ decay-in-flight and (5) dimuon pair produced through the Drell-Yan process. The fit result is shown in Fig. 1 (a) and (Data - Fit)/ Fit is shown in Fig. 1 (b). They observe 56 events in the search window, while $68 \pm 2(\text{stat.}) \pm 4(\text{syst.})$ are expected from the fit. There is no evidence of an excess of events due to the $b \to X_s\mu^+\mu^-$. Using the number of $b \to J/\psi X$ decay events for normalization, 90% confidence level upper limit for the branching fraction of the $b \to X_s\mu^+\mu^-$ decay is calculated,

[a] Present Address: High Energy Accelerator Research Organization, 1-1 Oho, Tsukuba Ibaraki 305-0801, Japan

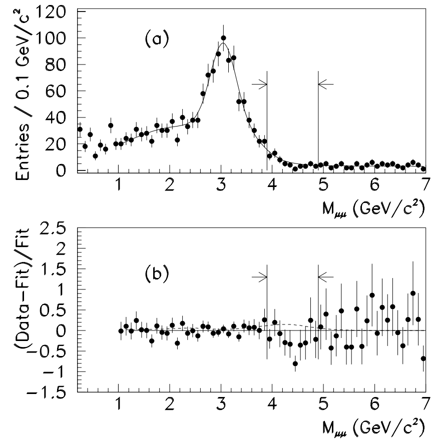

Figure 1: (a) Dimuon invariant mass spectrum. The solid line is the fit result. (b)(Data - Fit)/Data. The dashed line corresponds to 90% confidence level upper limit for th decay $b \to X_s\mu^+\mu^-$ from the fit.

and $\mathcal{B}(b \to X_s\mu^+\mu^-) < 3.2 \times 10^{-4}$. The Standard Model prediction [1] for the branching fraction is $(5.7 \pm 1.2) \times 10^{-6}$ and the best limit [3] is obtained by CLEO, $\mathcal{B}(b \to X_s\mu^+\mu^-) < 5.8 \times 10^{-5}$ [b].

1.2 Search for Exclusive FCNC decays $B \to K^{(*)}\mu^+\mu^-$ in CDF

The search for the exclusive FCNC decays, $B^+ \to K^+\mu^+\mu^-$ and $B^0 \to K^{*0}\mu^+\mu^-$ ($K^{*0} \to K^+\pi^-$) are performed in data collected by the dimuon trigger. The data correspond to 90 pb^{-1}. Fully reconstructing B meson at CDF, we can take an advantage to reduce background significantly. The $K^{(*)}\mu^+\mu^-$ candidates must satisfy the following selection requirements: $p_T(K^{(*)}\mu^+\mu^-) > 6$ GeV/c, $|\eta(K^{(*)}\mu^+\mu^-)| < 1$, transverse decay length $L_{xy} > 400$ μm and isolation $I > 0.6$, where I is defined as the p_T of the $K^{(*)}\mu^+\mu^-$ candidates divided by the scalar sum of all charged tracks including $p_T(K^{(*)}\mu^+\mu^-)$, within a cone $\sqrt{\eta^2 + \phi^2} < 1$. To remove background further, the impact parameter significance for every single track is required to be greater than 2. The resonant part of dimuon mass, *i.e.* $\pm$200 MeV/c^2 (100 MeV/c^2), around the world average mass of J/ψ (ψ(2S)), is excluded in these searches.

For the $B^+ \to K^+\mu^+\mu^-$ decay mode, the $K^+\mu^+\mu^-$ invariant mass is shown in Fig. 2. The top plot in Fig. 2 shows the mass distribution for the resonant $\mu^+\mu^-$ mass and the bottom one is for the non-resonant. The $K^{*0}\mu^+\mu^-$ invariant mass distribution for the resonant decay and for the non-resonant decay are also shown in Fig. 2. The $K^{(*)}\mu^+\mu^-$ signal region is defined as $|m(K^{(*)}\mu^+\mu^-) - m(B)| < 50$ MeV/c^2, where $m(B)$ is the world average B meson mass. The high mass region $100 < m(K^{(*)}\mu^+\mu^-) - m(B) < 600$ MeV/c^2 is used for the background region, since there exist events due to true $B \to J/\psi X$ decays in the lower mass region. For the resonant decays (Fig. 2 tops), we find a significant peak in the signal region, while few events in the background region. For the non-resonant decays (Fig. 2 bottoms), 4 candidates and 4 backgrounds are found in the $B^+ \to K^+\mu^+\mu^-$ mode. No candidate and 2 backgrounds are found in the B^0 $K^{*0}\mu^+\mu^-$ mode. From the Standard Model prediction for the branching fractions, we can expect 0.6 events of the $B^0 \to K^{*0}\mu^+\mu^-$ decays in the signal region using the number of the $B^0 \to K^{*0}\psi$ decays for normalization.

We see no excess due to the FCNC decay in each mode. Without background subtraction, we obtain the 90% C.L. upper limit for the branching fractions: $\mathcal{B}(B^+ \to K^+\mu^+\mu^-) < 5.4\times10^{-6}$ and $\mathcal{B}(B^0 \to K^{*0}\mu^+\mu^-) < 4.1\times10^{-6}$, while the Standard Model predictions [1] are $(0.4\pm1.5)\times10^{-6}$

[b] CLEO also obtained the 90% C.L. limit for the branching fraction, $\mathcal{B}(b \to X_s e^+e^-) < 5.7\times10^{-5}$. Combining the dielectron and dimuon decay modes, they found $\mathcal{B}(b \to X_s\ell^+\ell^-) < 4.2\times10^{-5}$.

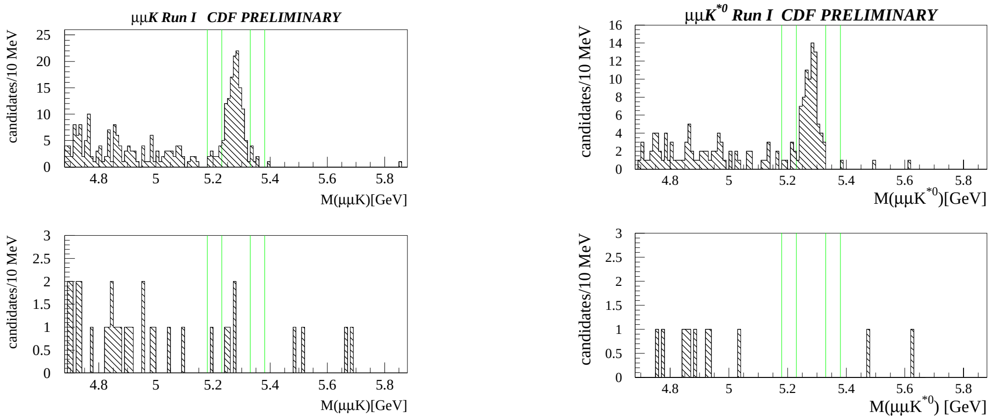

Figure 2: $K^{(*)}\mu^+\mu^-$ invariant mass distribution. Left: for $B^+ \to K^+\mu^+\mu^-$ resonant decay (top) and non-resonant decay (bottom). Right: for $B^0 \to K^{0*}\mu^+\mu^-$ resonant decay (top) and non-resonant decay (bottom).

and $(1.5 \pm 0.6) \times 10^{-6}$, respectively. These results are the most strict limits.

2 Observation of B_c^+ Mesons in CDF

The B_c^+ meson is a bound state of $\bar{b}$ quark and c quark. The Standard Model predicts an existence of the B_c^+ meson. The top quark is so heavy that it can not form a meson with a quark, and therefore, the B_c^+ meson is the heaviest meson consisting of different flavored quarks.

The B_c^+ production is expected to be 10^{-3} of $b\bar{b}$ production, according to pertuvative QCD calculations at α_s^4 order [4]. The mass for the ground state of $\bar{b}c$ is expected to be 6.258±0.020 GeV/c^2 with in the frame work of nonrelativistic QCD potential models[5]. Since the B_c^+ meson has flavors, it decays only via weak interaction. The predictions for the B_c^+ lifetimes lie in a wide range: $0.3 < \tau < 1.4$ ps, due to the assumption of the bound state effect [6].

LEP [7] and CDF [8] searched for the B_c^+ meson, but it was not observed previously.

2.1 Event Selection and Background Estimation

CDF searches for $B_c^+ \to J/\psi \ell^+ X$ ($\ell = e$ or μ), where $J/\psi \to \mu^+\mu^-$, in dimuon-trigger data (110 pb^{-1}).[9] We select $J/\psi \to \mu^+\mu^-$ events that both muon tracks are reconstructed in SVX. We find about 196000 $J/\psi \to \mu^+\mu^-$ events and apply the dimuon mass window cut $|(\mu^+\mu^-) - m(J/\psi)|$ < 50 MeV/c^2, where $m(J/\psi)$ is the world average J/ψ mass. In the dimuon mass window, we search for third lepton e with $p_T > 2$ GeV/c or μ with $p_T > 3$ GeV/c, where the third lepton and J/ψ are in the same hemisphere. The three leptons (μ^+, μ^-, ℓ) are required to form a good common vertex. Since there is missing momentum due to ν in the semileptonic decay mode, we can not fully reconstruct B_c^+ momentum and mass. From the Monte carlo simulation, the mass of J/ψ and third lepton ℓ system lies between 4 GeV/c^2 and 6 GeV/c^2 for a B_c^+ signal. Therefore, the signal region is defined as $4 < m(J/\psi\ell) < 6$ GeV/c^2. To remove prompt J/ψ events, we apply the pseudo-proper decay length $ct^* = \dfrac{m(J/\psi\ell)}{p_T(J/\psi\ell)} L_{xy} > 60$ μm cut, where L_{xy} is the transverse decay length. Fig. 3 (a) shows the J/ψ + 'track' mass distribution, where 'track' only satisfies the lepton fiducial requirements and is not applied other lepton identification requirements. These distributions are used in the various background estimation. Figs. 3 (b) show the $J/\psi + \ell$ mass distribution. We find 19 $J/\psi + e$ events and 12 $J/\psi + \mu$ events for $4 <$ $m(J/\psi\ell) < 6$ GeV/c^2.

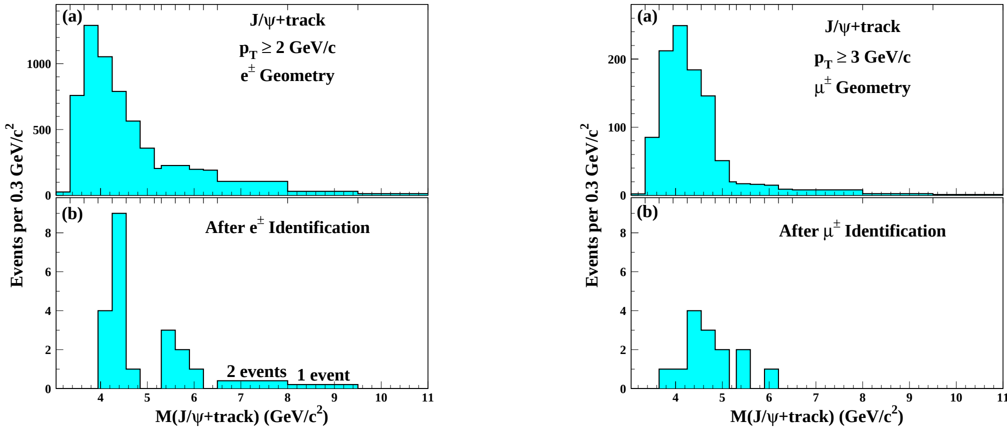

Figure 3: The mass distribution for J/ψ + track (a), where 'track' just satisfies the fiducial requirements, and for J/ψ + ℓ (b). Left: J/ψ + e. Right: J/ψ + μ.

Table 1: Summary of Counting Experiments

	$4.0 < M(J\psi\,\ell) < 6.0$ GeV$/c^2$	
	J/ψ e results	J/ψ μ results
Misidentified leptons		
Fake Electrons	$2.6 \pm 0.05 \pm 0.3$	
Conversions	$1.2 \pm 0.8 \pm 0.4$	
Punch-through		$0.88 \pm 0.13 \pm 0.33$
Decay-in-flight		$5.5 \pm 0.5 \pm 1.3$
$b\bar{b}$ bkg.	1.2 ± 0.5	0.7 ± 0.3
Total Background	5.0 ± 1.1	7.1 ± 1.5
Events observed in data	19	12
Net Signal	14.0	4.9
Combined	18.9	
$P_{Counting}$(Null)	2.1×10^{-5}	0.084

We identify and estimate the following background sources. For the electron mode, the dominant background sources are (i) fake electron background due to hadrons (π or K) misidentified as electrons, (ii) residual conversion background due to electrons unidentified by the conversion electron finding algorithm, and (iii) $b\bar{b}$ background due to events that J/ψ comes from one $\bar{b}$ and e from other b. The dominant backgrounds for the muon mode are (i) punch-through background due to hadrons that transverse without interacting in the calorimeter and hit a muon chamber, (ii) decay-in-flight background due to hadrons that decay into muons in front of muon chambers, and (iii) $b\bar{b}$ background. We show the amounts of these backgrounds and the summary of counting experiment in Table 1. We see some excesses in both modes and discuss a magnitude of significance for the excesses in the next section.

2.2 Statistical Significance of Signal

To test a statistical significance for the apparent excess, we perform mass shape analysis. We fit the observed $J/\psi\ell$ mass distribution from 3.35 to 11.0 GeV$/c^2$ using a binned likelihood method. The signal shape is obtained from Monte Carlo simulation for the $B_c^+ \to J/\psi\ell^+\nu$ decay, and

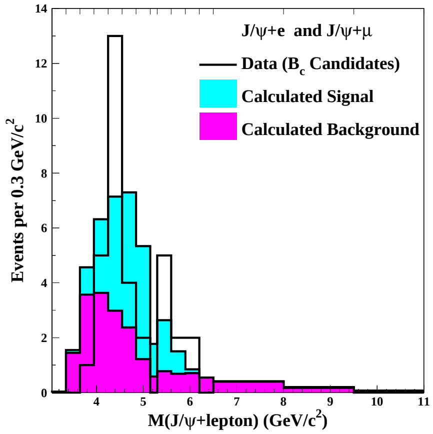

Figure 4: $J/\psi\ell$ mass distribution with the fit result.

each background shape that is discussed in the previous section is obtained from data and Monte Carlo simulation. In the fit, only the number of B_c signals is unconstrained parameters. Other parameters, such as the expected fraction of two modes, number of backgrounds and background shapes, are constrained by their uncertainties. We show the $J/\psi\ell$ mass distribution with the fit results in Fig. 4. From the fit, we found the number of B_c^+ signals $N(B_c^+)$ to be $20.4^{+6.2}_{-5.5}$.

We test a null hypothesis as follows. For each background, we allow the number of backgrounds to fluctuate with the estimated number of background and its uncertainty and obtain it to be N_b. Then we generate N_b backruond events according to the background mass distribution. We fit the mass distribution due to the only background contribution, using same way as real data. From 351900 trials for this process, we estimate the number of the fit signals that are greater than $N(B_c^+) = 20.4$ for the data fit. We find the probability that a statistical fluctuation in the background can explain the excess in the data is estimated to be 6.3×10^{-7} that correspond to 4.8 standard deviations in significance. In the next section, we estimate the basic properties, such as mass, lifetime and cross section ratio, assuming that the observed excesses are due to the existence of the B_c^+ meson.

2.3 Measurement of the B_c^+ properties Mass, Lifetime and Cross section Ratio

The B_c^+ meson mass is estimated using the same fitting technique. We fit $m(J/\psi\ell)$ distribution with varying the assumed B_c^+ mass templates in the range 5.52 to 7.52 GeV/c^2. The relative log-likelihood $\xi_m = -2\ln\left(\frac{\mathcal{L}(m)}{\mathcal{L}(m=6.40)}\right)$, at each assumed B_c^+ mass, and ξ_m as a function of an assumed B_c^+ mass is shown in Fig. 5. From the minimum ξ_m, the B_c^+ mass is estimated to be $6.40 \pm 0.39(\text{stat.}) \pm 0.13(\text{syst.})$ GeV/c^2.

We changed the $ct^* > 60$ μm to $ct^* > -100$ μm cut in order to estimate the lifetime using the entire ct^* distribution. Since we can not fully reconstruct the B_c^+ mass and momentum event by event due to the missing momentum, we correct for the missing momentum using Monte Carlo simulation. The relation between ct^* and proper decay length ct is given by $ct^* = \frac{ct}{K}$, where $K = \frac{m(B_c^+)}{m(J/\psi\ell^+)} \times \frac{p_T(J/\psi\ell^+)}{p_T(B_c^+)}$. We obtain the K distribution from the Monte Carlo simulation and convolute an exponential tail with the K distribution in the signal shape. We also obtain the ct^* distribution for backgrounds discussed in Section 2.1. Then we fit the observed ct^* distribution to a sum of signal and background, using an unbinned likelihood method. The ct^* distribution is shown in Fig. 5 with the lifetime fit result. The B_c^+ lifetime is measured to be

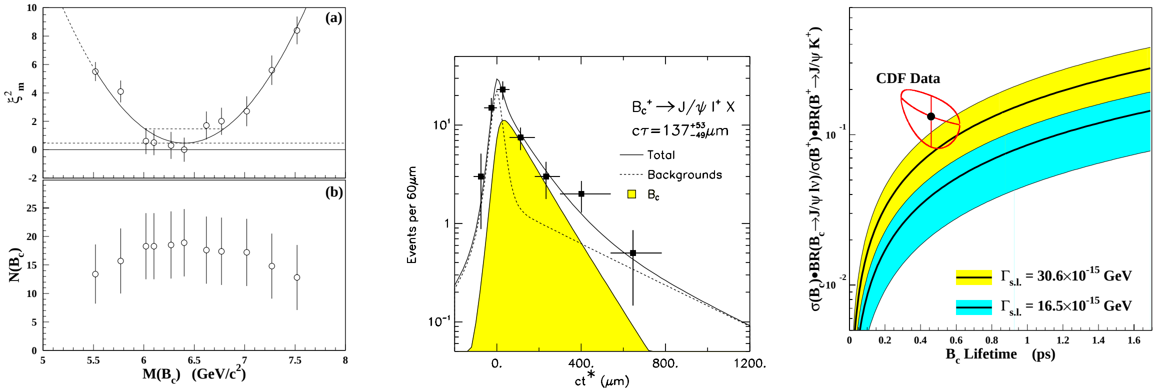

Figure 5: Left: ξ^2_m (a) and $N(B_c^+)$ (b) as a function of an assumed B_c^+ mass. Middle: ct^* distribution with the lifetime fit result. Right: $\sigma\mathcal{B}$ ratio as a function of the observed B_c^+ lifetime. The shaded regions are theoretical predictions with the two different partial width.

$0.46^{+0.18}_{-0.16}$(stat.)$\pm$0.03(syst.) ps.

We measured the cross section ratio of $\sigma(B_c^+)\mathcal{B}(B_c^+ \to J/\psi\ell^+\nu)$ to $\sigma(B_u^+)\mathcal{B}(B_u^+ \to J/\psi K^+)$. The event topology for the $B_u^+ \to J/\psi K^+$ is very similar to that for the B_c^+ semileptonic decay. Therefore, many systematic uncertainties are canceled in the ratio. The ratio is estimated to be $0.132^{+0.041}_{-0.037}$(stat.)$\pm$0.031(syst.)$^{+0.032}_{-0.020}$(lifetime) and the ratio as a function of the measured lifetime is shown in Fig. 5.

3 Conclusions

In the Tevatron experiments, the search for the FCNC decays $b \to s\mu^+\mu^-$ were performed. The signal for the decays has not been seen yet.

CDF observed the B_c^+ meson through the $B_c^+ \to J/\psi\ell^+X$ mode. We find $20.4^{+6.2}_{-5.5}$ B_c^+ signals from the the $J/\psi\ell$ mass fit. A fit without B_c^+ contribution is rejected at the level of 4.8 standard deviations. Then we measured the B_c^+ properties:

- mass: 6.40 ± 0.39(stat.)$\pm$0.13(syst.) GeV/c^2,
- lifetime: $0.46^{+0.18}_{-0.16}$(stat.)$\pm$0.03(syst.) ps,
- $\sigma\mathcal{B}$ ratio: $0.132^{+0.041}_{-0.037}$(stat.)$\pm$0.031(syst.)$^{+0.032}_{-0.020}$(lifetime).

References

1. A. Ali, DESY 97-019, hep-ph/97022312.
2. B. Abbot *et al*, *Phys. Lett.* B **423**, 419 (1998).
3. CLEO Collaboration, CLNS 97/1514, hep-ex/971003.
4. C.H. Chang, Y.Q. Chen and R.J. Oakes, *Phys. Rev.* D **54**, 4344 (1996); M. Lusignoli, M. Masetti and S. Petrarca, *Phys. Lett.* B **266**, 142 (1991).
5. E.J. Eichten and C. Quigg, *Phys. Rev.* D **49**, 5484 (1994).
6. C. Quigg, FERMILAB-CONF-93/265-T; I.I. Bigi, *Phys. Lett.* B **371**, 105 (1996); M. Beneke and G. Buchalla, *Phys. Rev.* D **49**, 4991 (1996).
7. R. Barate *et al*, *Phys. Lett.* B **402**, 213 (1997); P. Abreu *et al*, *Phys. Lett.* B **398**, 207 (1997); G. Alexaunder *et al*, *Phys. Lett.* B **420**, 157 (1998).
8. F. Abe *et al*, *Phys. Rev. Lett.* **77**, 5176 (1996).
9. F. Abe *et al*, FERMILAB-PUB-98-121-E, submitted to *Phys. Rev.* D.